https://doi.org/10.17221/18/2026-CJGPB

Quantum-inspired machine learning for screening PEG-induced drought stress responses in caraway (*Carum carvi* L.)

Samuel Goitom Misginna[1], *Omar Gaoua*[1], *Petra Röszlerová*[1,2], *Musab A. Isak*[3], *Ondřej Hejna*[1], *Patrick Kamulegeya*[1], *Eva Jozová*[1], *Vladislav Čurn*[1]*

[1]*Department of Genetics and Biotechnology, Faculty of Agriculture and Technology, University of South Bohemia, České Budějovice, Czech Republic*
[2]*Institute of Laboratory Diagnostics and Public Health, Faculty of Health and Social Sciences, University of South Bohemia, Czech Republic*
[3]*Department of Agricultural Sciences and Technology, Faculty of Graduate School of Natural and Applied Sciences, Erciyes University, Kayseri, Türkiye*

**Corresponding author: curn@fzt.jcu.cz*

Citation: Misginna S.G., Gaoua O., Röszlerová P., Isak M.A., Hejna O., Kamulegeya P., Jozová E., Čurn V. (2026): Quantum-inspired machine learning for screening PEG-induced drought stress responses in caraway (*Carum carvi* L.). Czech J. Genet. Plant Breed., 62: 170–189.

Abstract: Drought is a significant factor limiting the growth and early establishment of caraway (*Carum carvi* L.), a valuable medicinal and aromatic plant. In this study, polyethylene glycol (PEG-6000)-induced osmotic stress assays were combined with statistical and machine learning (ML) approaches to assess early drought responses in five caraway cultivars and breeding materials. Seeds were subjected to four PEG concentrations (0, 5, 10 and 15 %), and key germination and seedling traits, including germination percentage (GP), root length (RL), root fresh weight (RFW), root dry weight (RDW), shoot height (SH), shoot fresh weight (SFW), and shoot dry weight (SDW), were measured. Higher PEG levels caused a sharp, accession-dependent decline in all traits, with germination dropping by 68 % at a 15 % PEG. Cultivars Aprim and H1b2/12 consistently showed better germination, shoot height, and biomass retention across stress levels, while Aklei exhibited lower germination but relatively stronger root growth, suggesting a differential adaptive response under osmotic stress. A linear model (LM) incorporating PEG concentration, accession, and their interaction served as the primary interpretable framework, explaining a large proportion of trait variation (R^2 = 0.81–0.94). Principal component analysis (PCA) and correlation analyses further revealed coordinated responses among biomass-related traits and differentiation in early-stage stress responses among accessions. Traditional ML models (MLP and SVR) were compared with quantum-inspired architectures (QiMLP and QiSVR); the quantum-inspired models showed comparable predictive performance in this dataset for certain traits, with QiMLP achieving the highest overall accuracy (R^2 = 0.88–0.94). This study presents an integrated phenotyping framework combining controlled stress assays with interpretable statistical modelling to evaluate early growth responses to PEG-induced drought stress in caraway. Overall, the results highlight accession-specific differences in early drought response and provide a useful basis for phenotyping and early-stage screening in caraway breeding.

Keywords: medicinal, aromatic and spice plants; neural networks; osmotic stress; predictive phenotyping; seedling traits

Supported by the University of South Bohemia, Czech Republic, Project No. GAJU 083/2025/Z and by the Ministry of Agriculture, Czech Republic, Project No. NAZV QL24010185.

https://doi.org/10.17221/18/2026-CJGPB

Caraway (*Carum carvi* L.) is a valuable annual or biennial aromatic plant of the Apiaceae family, grown worldwide for its essential oil-rich seeds that are extensively used in the food, pharmaceutical, and cosmetic industries (Bailer et al. 2001; Rasooli & Allameh 2016). Europe is one of the main production hubs for caraway, particularly in the Netherlands, Finland, Czech Republic and Poland, where cultivation of this crop supports both the spice trade and the essential oil industry (Bouwmeester & Smid 1995; Valkovszki & Németh-Zámbori 2011; von Maydell et al. 2020). The increasing global demand for caraway and its bioactive compounds highlights the need for resilient, stress-tolerant, and high-yielding cultivars (Aly et al. 2023; Agnihotri et al. 2024). However, the productivity of this species is increasingly threatened by abiotic stresses, particularly drought, which is expected to intensify and occur more frequently due to ongoing climate change (Ahluwalia et al. 2021; Mittler et al. 2025). Drought stress is one of the most detrimental abiotic factors affecting aromatic and medicinal plants, causing significant reductions in biomass, seed yield, and essential oil production (Ahluwalia et al. 2021; Seleiman et al. 2021). In caraway, water shortage markedly reduces photosynthetic activity, seed production, and essential oil yield, and alters the composition of major monoterpenes such as carvone and limonene (Laribi et al. 2009). Recent studies in arid and semi-arid regions have further revealed that the caraway germination percentage, root elongation, and seedling dry weight decrease under water deficit, highlighting the species' pronounced sensitivity during early developmental stages (Nezamivand et al. 2021). Early seedling vigour under moisture-limited conditions is therefore crucial for successful field establishment and yield stability (Kaya et al. 2006; Almaghrabi 2012).

To simulate drought conditions under controlled environments, polyethylene glycol (PEG-6000) is widely used due to its ability to reduce water potential without penetrating plant tissue, providing a reproducible and standardised method for imposing osmotic stress (Money 1989; Verslues et al. 2006; Licaj et al. 2024). PEG-induced water deficit triggers physiological and biochemical responses, including osmotic adjustment, reduced cellular expansion, reactive oxygen species (ROS) accumulation, and increased antioxidant activity, mechanisms that mirror natural drought responses in diverse plant species (Sharma et al. 2022; Ema et al. 2025). Genotype-dependent variation in these responses is well documented in cereals and medicinal plants, suggesting strong potential for early-stage drought screening using PEG assays (Mirmazloum et al. 2020; Othmani et al. 2021).

The inherent complexity of these multi-dimensional datasets, however, necessitates advanced analytical approaches. Machine learning (ML) has thus become a crucial tool for modelling complex, nonlinear plant responses, especially in drought and PEG-induced stress studies, where genotype × environment interactions are hard to capture with traditional statistics (Kamilaris & Prenafeta-Boldú 2018; Liakos et al. 2018). Recent applications of multi-layer perceptron (MLP), general regression neural network (GRNN), and support vector machine (SVM) models in *in vitro* systems have shown superior predictive performance for stress-related traits compared to classical methods (Rezaei et al. 2023). Similarly, ensemble algorithms such as random forest (RF), XGBoost, and Stacking Regression (SR) have achieved high accuracy in predicting morphogenic traits in *Punica granatum* and *Aronia melanocarpa* micropropagation, especially when optimised using evolutionary algorithms like NSGA-II (Zarbakhsh et al. 2024; Yaman et al. 2025). In PEG-based drought experiments, ML has been effective in detecting subtle genotype-specific responses; for example, RF exceeded 90 % accuracy in predicting PEG-induced drought tolerance patterns in strawberry (Şimşek 2024). These results highlight ML's ability to uncover hidden patterns from multivariate datasets and identify key traits related to drought resilience. Emerging quantum-inspired models, such as quantum-inspired multilayer perceptron (QiMLP), further enhance these capabilities by improving feature-correlation learning and managing complex nonlinearities (Zhang et al. 2025).

Despite the recognised sensitivity of caraway to drought, accession-specific early-stage responses to PEG-induced osmotic stress remain insufficiently characterised within a framework directly relevant to phenotyping and breeding. Consequently, breeders still lack a quantitative framework for identifying accessions with improved stress resilience during early growth. To address this gap, the present study (*i*) evaluated the effects of graded PEG-induced osmotic stress on germination and seedling traits in five *C. carvi* accessions; (*ii*) quantified accession-specific variation in root and shoot growth and biomass accumulation; and (*iii*) applied machine learning algorithms to predict stress-related morphophysiological traits and identify accessions exhibiting stronger early-stage resilience under osmotic stress conditions.

https://doi.org/10.17221/18/2026-CJGPB

MATERIAL AND METHODS

Plant material. The seeds of three Czech *C. carvi* cultivars (Aprim, Aklei, Kamin) and two breeding materials (4a/1 and H1b2/12) were obtained from a regional agricultural breeding and research centre (Agritec Plant Research s.r.o., Czechia/Šumperk). All seeds were harvested in 2024 and were stored in a dry, cool environment at 4 °C prior to experimentation to maintain viability. Although additional seed viability assays, such as tetrazolium testing, were not performed prior to the experiment, all accessions were provided as certified breeding materials from the same source. Therefore, differences observed in germination under control conditions are attributable to inherent accession variation rather than differences in seed lot quality. Before use, seeds were rinsed under running tap water for 5 minutes and surface-sterilised with 70% ethanol for 30 seconds. Next, seeds were immersed in 1% (v/v) sodium hypochlorite for 3 minutes. Finally, the seeds were rinsed three times with sterile distilled water and air-dried on sterile filter paper inside a laminar flow hood.

PEG solution preparation. Drought stress was simulated using polyethylene glycol 6000 (PEG-6000, Sigma-Aldrich, Germany) solutions at three concentrations: 5%, 10%, and 15% (w/v), along with a 0% PEG control. The selected PEG concentrations represent a gradient from mild to severe osmotic stress commonly used in controlled drought simulation studies. PEG-6000 solutions in the range of 5–15% have been widely applied to impose progressive reductions in water potential during germination assays, enabling the identification of both moderate stress responses and tolerance thresholds in seedlings (Verslues et al. 2006; Bayoumi et al. 2008; Sharma et al. 2022). The pH of each solution was adjusted to 5.8 using 1 N NaOH or 1 N HCl.

Experimental design. A completely randomised design (CRD) was used with four PEG treatments and five accessions, resulting in a 4 × 5 factorial arrangement. Each treatment consisted of three biological replicates, with 40 seeds per replicate (n = 120 seeds per treatment). Seeds were placed on sterile 90 mm Petri dishes (Isolab, Germany) lined with two layers of Whatman No. 1 filter paper moistened with exactly 5 mL of the corresponding PEG solution. Petri dishes were sealed with parafilm to minimise moisture loss and incubated at 25 ± 1 °C, 60% relative humidity, and 16/8 h light/dark photoperiod for 15 days in a controlled-environment growth chamber (Sanyo MLR 352/H, Sanyo Electric, Japan). Seedling traits were measured at the Petri dish level, and representative values were recorded for each accession × PEG treatment replicate rather than retaining individual-seed measurements.

Morphological data collection. At the end of the incubation period, a set of morphological traits was evaluated to quantify the seedlings' responses to drought stress. Germination percentage was determined as the ratio of germinated seeds to the total number of sown seeds. Root and shoot lengths were measured using a ruler, and the fresh biomass of both organs was recorded immediately after excision. To determine dry weight, seedlings were dried in a hot air oven at 70 °C for 7 h and subsequently weighed. These traits were selected because they serve as well-established and reliable indicators of early-stage drought tolerance in seedling assays (Sharma et al. 2022). These morphometric traits are widely used as early indicators of drought sensitivity because they directly reflect seedling establishment and growth performance under osmotic stress conditions. Germination and early seedling growth responses are particularly informative during the initial stages of drought screening, where rapid phenotypic differences among genotypes can be detected under controlled conditions.

Statistical analysis. Data were assessed for normality using the Shapiro-Wilk test and for homogeneity of variances using Levene's test. A two-way ANOVA was conducted to examine the effects of PEG level, accession, and their interaction. When significant differences were detected, mean separation was performed using Tukey's least significant difference (LSD) test at a significance threshold of $P < 0.05$. In addition to significance testing, effect sizes were estimated using eta-squared (η^2) values to quantify the proportion of variance explained by PEG level, accession, and their interaction. All statistical analyses were performed in R (version 4.3) using the 'stats', 'car', and 'agricolae' packages. Principal component analysis (PCA) and Pearson correlation analysis were also conducted in R using the 'FactoMineR', 'factoextra', and 'corrplot' packages to visualise multivariate trait relationships and identify patterns associated with drought stress. Graphical outputs were generated using 'ggplot2'.

Modelling procedure. In addition to ANOVA, an interpretable linear model was fitted separately for each measured trait using PEG concentration, accession, and their interaction (PEG × accession) as predictors. This model structure was selected

https://doi.org/10.17221/18/2026-CJGPB

because it directly reflects the factorial experimental design and allows straightforward interpretation of treatment, genotype, and interaction effects on germination and seedling-growth responses. Estimated coefficients and 95% confidence intervals were visualised to assess the magnitude and direction of PEG, accession, and interaction effects across traits. Four modelling frameworks were implemented for comparative evaluation: the basic multi-layer perceptron (MLP), the basic support vector regression (SVR), and their quantum-inspired counterparts (QiMLP and QiSVR). All modelling analyses were conducted in MATLAB (MathWorks Inc.). The dataset comprised two input variables, accessions and PEG concentrations, and seven continuous output parameters representing plant growth and stress indicators: germination percentage (GP), root length (RL), shoot height (SH), root fresh weight (RFW), shoot fresh weight (SFW), root dry weight (RDW), and shoot dry weight (SDW). Because the dataset was derived from a controlled laboratory experiment with a limited number of treatment combinations, the machine learning models are primarily intended to explore predictive relationships among genotype, PEG level, and growth traits rather than to serve as large-scale predictive systems. The categorical variable "Accession" was encoded numerically as a categorical identifier for model input representation. Because accessions represent independent genotypic categories rather than ordinal variables, the encoding does not imply any ordered biological relationship among genotypes. Numerical variables were standardised using z-score normalisation. All the data were randomly partitioned into 80% for training and 20% for testing using a fixed random seed (rng = 42) to ensure reproducibility. Because the dataset originates from a controlled factorial experiment with a limited number of treatment combinations, model stability was further examined through repeated training runs to minimise potential bias associated with a single random partition.

The basic MLP architecture consists of an input layer followed by two fully connected hidden layers with 25 and 10 neurons, each employing a Rectified Linear Unit (ReLU) activation function, and a single regression output layer. The network was trained using the *Adam* optimiser. For the BasicSVR models, an ε-SVR formulation was applied with a Gaussian radial basis function (RBF) kernel, a box constraint (C) of 1.0, an epsilon value of 0.1, and automatic kernel scaling. The advanced models utilised quantum-inspired feature encoding to enhance their representational capacity. In the *QiMLP*, each input variable was transformed into four quantum-derived features simulating phase, amplitude, and interference encodings: $\cos(\pi x_{\text{norm}})$, $\sin(\pi x_{\text{norm}})$, $\sqrt{1 - x^2}_{\text{norm}}$ and $\cos(2\pi x_{\text{norm}}) \sin(\pi x_{\text{norm}})$, where x_{norm} is the min–max normalised input.

QiSVR extends this mapping by incorporating an additional set of interaction features inspired by quantum entanglement, defined as $\sin(\pi x_{1,\text{norm}}) \cos(\pi x_{2,\text{norm}})$. Dropout regularisation was incorporated within the QiMLP architecture to reduce the risk of overfitting given the relatively compact dataset size. The QiMLP model architecture consisted of quantum-encoded inputs feeding two hidden layers of 32 and 16 neurons (powers of two, reflecting qubit-inspired dimensionality), with *tanh* and *ReLU* activations, dropout rates of 0.15 and 0.10, and trained using the *Adam* optimiser with a stepwise learning rate decay schedule. The *QiSVR* uses the same RBF kernel configuration as the baseline but operates on the quantum-enhanced feature space. The purpose of the quantum-inspired feature transformation is not to emulate physical quantum computation but to enrich the input representation through nonlinear trigonometric mappings that increase the expressive capacity of classical machine learning models. Model performance was assessed using denormalised predictions from both the training and independent test datasets using three statistical indices: the coefficient of determination (R^2) (Equation 1), root mean squared error (RMSE) (Equation 2) and mean absolute error (MAE) (Equation 3). Additionally, diagnostic plots-actual versus predicted relationships and support vector statistics were generated to visualise the predictive accuracy and model complexity. Model performance was evaluated using both training and test datasets. While Table 3 reports the training performance metrics, Figures 7 and 8 illustrate the agreement between actual and predicted values for both datasets, enabling visual assessment of model generalisation.

$$R^2 = 1 - \frac{\sum_{i=1}^{n}(Y_i - \hat{Y}_i)^2}{\sum_{i=1}^{n}(Y_i - \tilde{Y})^2} \quad (1)$$

$$\text{RMSE} = \sqrt{\frac{\left(\sum_{i=1}^{n}(Y_i - \hat{Y}_i)^2\right)}{n}} \quad (2)$$

$$\text{MAE} = \frac{1}{n}\sum_{i=1}^{n}|Y_i - \hat{Y}_i| \quad (3)$$

https://doi.org/10.17221/18/2026-CJGPB

RESULTS

Influence of PEG-induced drought stress on the growth parameters of different *Carum carvi* cultivars and breeding materials. PEG-induced drought stress affects germination and early seedling growth in five *C. carvi* accessions (Table 1). As the PEG concentration increased from 0% to 15%, there was a consistent and significant decline ($P < 0.001$) in several key metrics: GP, RL, SH, and both fresh- and dry-biomass traits: RFW, SFW, RDW, and SDW. Under control conditions (0% PEG), the highest germination rates were recorded for the cultivar Aprim (69.17%) and H1b2/12 (65.50%). In contrast, the Aklei cultivar presented a significantly lower germination rate (20.83%). All the cultivars and breeding materials showed a significant decrease in germination rates at 15% PEG. While the germination rates for Aprim and Kamin reached 25.0% and 20.0%, respectively, Aklei (10.0%) and 4a/1 (15.0%) exhibited significantly lower values. A similar inhibitory trend was observed for the elongation of roots and shoots. Aklei had the longest roots (7.31 cm) at 0% PEG, while Aprim (5.97 cm) and H1b2/12 (3.37 cm) produced moderately long roots. The root length decreased drastically when the PEG content was increased to 15%; the reduction was 70–80%, resulting in a root length of 1.71 cm in Aprim, 0.84 cm in Kamin, and 0.64 cm in 4a/1. Additionally, shoot height was also significantly reduced; at 15% PEG, it decreased from 3.86 cm for Aprim and 3.39 cm for Aklei under control conditions to 1.91 cm and 1.18 cm, respectively. Fresh and dry biomass metrics demonstrated the cumulative effects of stress on plant vigour. 4a/1 had the highest shoot fresh weight (12.54 g) and shoot dry weight (2.39 g) among the unstressed plants. Aprim came in second with 12.37 g and 2.49 g, and Kamin with 11.88 g and 2.48 g. These values sharply decreased under extreme stress (15% PEG); Aprim's shoot fresh weight fell to 4.42 g

Table 1. Influence of polyethylene glycol (PEG)-induced drought stress on growth parameters in different *Carum carvi* accessions

Accession	PEG (%)	GP	RL	SH	RFW	SFW	RDW	SDW
Aprim	0	69.17 ± 8.20^{a}	5.97 ± 0.47^{b}	3.86 ± 0.17^{a}	8.11 ± 0.29^{a}	12.37 ± 0.39^{a}	1.56 ± 0.09^{cd}	2.49 ± 0.25^{a}
	5	45.00 ± 4.33^{c}	4.10 ± 0.14^{cd}	3.17 ± 0.19^{bc}	6.29 ± 0.55^{cde}	10.49 ± 0.39^{cd}	1.28 ± 0.08^{ef}	1.58 ± 0.24^{ef}
	10	35.83 ± 1.25^{e}	2.99 ± 0.15^{fgh}	2.54 ± 0.15^{d}	4.46 ± 0.35^{hi}	9.07 ± 0.64^{ef}	0.93 ± 0.10^{g}	0.92 ± 0.14^{j}
	15	25.00 ± 4.33^{fg}	1.71 ± 0.27^{k}	1.91 ± 0.26^{gh}	3.11 ± 0.23^{jk}	4.42 ± 0.60^{ij}	0.61 ± 0.20^{h}	0.47 ± 0.12^{kl}
Aklei	0	20.83 ± 1.25^{gh}	7.31 ± 0.44^{a}	3.39 ± 0.42^{b}	6.91 ± 0.33^{bc}	10.16 ± 0.24^{cde}	2.59 ± 0.24^{a}	1.73 ± 0.12^{de}
	5	14.17 ± 1.25^{jk}	6.07 ± 0.42^{b}	2.41 ± 0.38^{de}	5.84 ± 0.22^{def}	5.92 ± 0.29^{h}	1.80 ± 0.12^{b}	1.31 ± 0.11^{h}
	10	15.00 ± 2.17^{ijk}	4.33 ± 0.34^{c}	1.97 ± 0.21^{fg}	4.06 ± 0.27^{i}	5.08 ± 0.27^{hi}	1.20 ± 0.12^{f}	1.04 ± 0.13^{ij}
	15	10.00 ± 2.17^{k}	2.77 ± 0.38^{ghi}	1.18 ± 0.32^{j}	3.08 ± 0.26^{k}	3.73 ± 0.35^{j}	0.63 ± 0.16^{h}	0.59 ± 0.23^{k}
Kamin	0	55.83 ± 4.51^{b}	3.23 ± 1.07^{fg}	2.93 ± 0.17^{c}	7.67 ± 0.30^{ab}	11.88 ± 0.42^{ab}	1.41 ± 0.13^{de}	2.48 ± 0.22^{a}
	5	45.83 ± 2.50^{c}	2.19 ± 0.73^{jk}	2.37 ± 0.19^{de}	7.33 ± 0.13^{ab}	10.51 ± 0.31^{cd}	1.13 ± 0.32^{f}	1.54 ± 0.09^{fg}
	10	29.17 ± 4.51^{f}	1.71 ± 0.50^{k}	1.98 ± 0.20^{fg}	6.43 ± 0.23^{cd}	4.58 ± 0.49^{ij}	0.67 ± 0.07^{h}	0.89 ± 0.23^{j}
	15	20.00 ± 2.17^{ghi}	0.84 ± 0.28^{lm}	0.32 ± 0.10^{k}	4.44 ± 0.68^{hi}	2.54 ± 0.22^{k}	0.33 ± 0.10^{i}	0.41 ± 0.08^{l}
4a/1	0	59.09 ± 8.31^{b}	3.75 ± 0.53^{de}	2.25 ± 0.49^{def}	4.97 ± 1.66^{gh}	12.54 ± 2.01^{a}	1.81 ± 0.12^{b}	2.39 ± 0.13^{a}
	5	41.67 ± 3.31^{cd}	3.26 ± 0.62^{f}	1.96 ± 0.44^{fg}	5.56 ± 1.47^{efg}	9.50 ± 3.54^{de}	1.70 ± 0.14^{bc}	2.07 ± 0.18^{c}
	10	35.25 ± 2.19^{e}	2.47 ± 0.35^{ij}	1.63 ± 0.59^{hi}	5.21 ± 2.30^{fgh}	8.18 ± 2.02^{fg}	1.15 ± 0.11^{f}	1.75 ± 0.08^{d}
	15	15.00 ± 2.17^{ijk}	0.64 ± 0.41^{m}	0.29 ± 0.09^{k}	2.16 ± 0.17^{l}	2.29 ± 0.26^{k}	0.74 ± 0.18^{h}	1.40 ± 0.21^{gh}
H1b2/12	0	65.50 ± 15.22^{a}	3.37 ± 0.81^{ef}	2.18 ± 0.52^{efg}	3.90 ± 0.77^{ij}	10.89 ± 1.73^{bc}	1.53 ± 0.17^{d}	2.46 ± 0.13^{a}
	5	56.00 ± 7.75^{b}	2.70 ± 0.71^{hi}	2.02 ± 0.61^{fg}	4.66 ± 1.41^{hi}	10.56 ± 1.64^{cd}	1.35 ± 0.25^{e}	2.23 ± 0.31^{b}
	10	37.50 ± 6.50^{de}	1.73 ± 0.50^{k}	1.44 ± 0.22^{ij}	2.84 ± 0.12^{kl}	7.66 ± 0.81^{g}	0.98 ± 0.17^{g}	1.56 ± 0.13^{fg}
	15	16.67 ± 3.31^{hij}	1.20 ± 0.15^{l}	1.31 ± 0.11^{j}	2.19 ± 0.20^{l}	5.92 ± 0.58^{h}	0.61 ± 0.14^{h}	1.10 ± 0.19^{i}

GP – germination percentage; RL – root length; SH – shoot height; RFW – root fresh weight; SFW – shoot fresh weight; RDW – root dry weight; SDW – shoot dry weight; LSD_{GP} – 5.016***; LSD_{RL} – 0.462***; LSD_{SH} – 0.304***; LSD_{RFW} – 0.784 ***; LSD_{SFW} – 1.098 ***; LSD_{RDW} – 0.143 ***; LSD_{SDW} – 0.162***; ***$P < 0.0001$; letters show statistical differences between caraway accessions, as determined by the least significant difference (LSD) analysis

https://doi.org/10.17221/18/2026-CJGPB

and shoot dry weight to 0.47 g. Similarly, root dry weight dropped in Aklei from 2.59 g to 0.63 g and in Aprim from 1.56 g to 0.61 g. Effect size analysis based on partial eta-squared values indicated that PEG level explained the largest proportion of variance across traits (η^2 = 0.70–0.92), followed by accession (η^2 = 0.45–0.84), while the accession × PEG interaction accounted for a moderate proportion of variance (η^2 = 0.33–0.547). These results indicate that drought stress intensity was the dominant factor shaping early seedling responses, although genotypic differences and their interaction with PEG level also contributed substantially to phenotypic variation.

Effect of different caraway accessions on growth parameters. Notable genotypic differences were observed among the five *C. carvi* accessions for all assessed growth characteristics (Figure 1). H1b2/12 (44.8%) and Aprim (43.8%) had the highest germination rates, indicating significant seed vigour and superior physiological preparedness for germination, while the GP varied considerably. Aklei, on the other hand, had the lowest germination rate (15.0%). It is interesting to note that, despite its poor germination rate, Aklei produced the longest roots (5.12 cm). Kamin recorded the shortest roots, measuring 1.99 cm, which suggests limited capacity for elongation or a reduced root development under stress conditions. In terms of shoot height, Aprim excelled, reaching a height of 2.86 cm, outperforming other accessions. In contrast, the 4a/1 and H1b2/12 breeding materials exhibited shorter shoots. The variations in fresh and dry biomass further highlight these different growth strategies. Kamin produced the highest root fresh weight at 6.46 g. In comparison, Aprim displayed the most significant shoot fresh weight at 9.09 g. Regarding dry weights, Aklei achieved the highest root dry weight of 1.56 g, indicating greater root development. Meanwhile, 4a/1 and H1b2/12 recorded the highest shoot dry weights at 1.92 g and 1.86 g, respectively, indicating greater shoot growth, which may reflect differences in growth allocation. Aprim showed relatively consistent perfor-

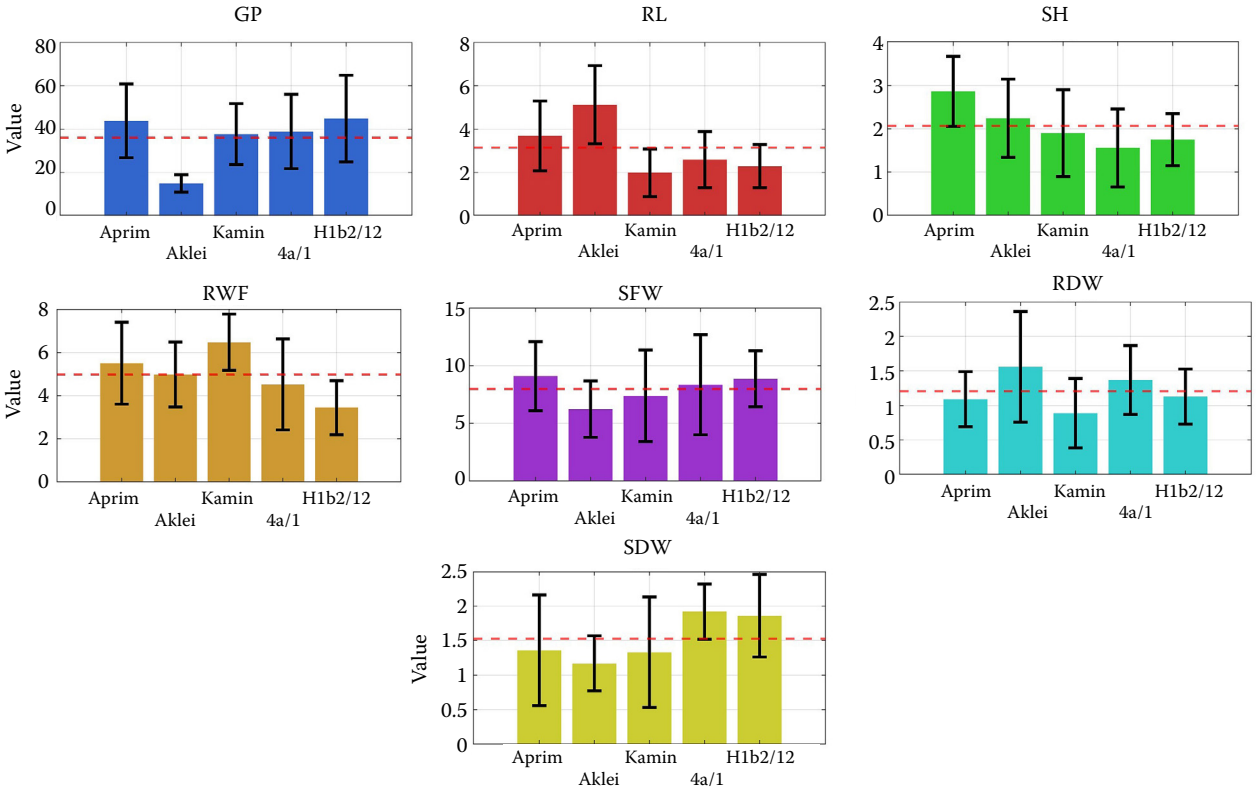

Figure 1. Effect of different *Carum carvi* accessions on germination and seedling growth parameters. Bars represent mean values averaged across all polyethylene glycol (PEG) treatments, and error bars indicate standard deviation (SD) of three biological replicates (n = 3)

The red dashed line denotes the overall mean across genotypes for each parameter: GP – germination percentage (%); RL – root length (cm); SH – shoot height (cm); RFW – root fresh weight (g); SFW – shoot fresh weight (g); RDW – root dry weight (g); SDW – shoot dry weight (g)

https://doi.org/10.17221/18/2026-CJGPB

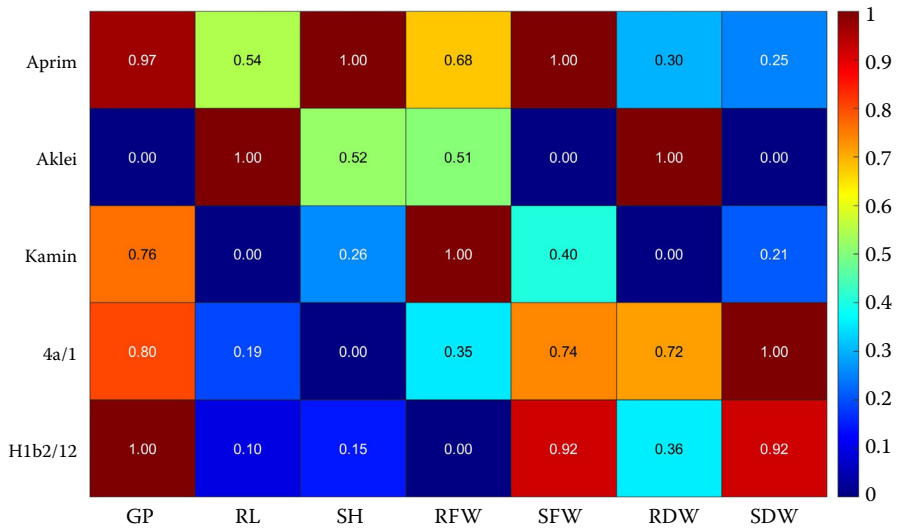

Figure 2. Normalised growth parameters across *Carum carvi* accessions; growth traits were normalised using min–max scaling (range: 0–1) to allow direct comparison among parameters with different measurement units

Values are dimensionless, where 0 represents the lowest observed value, and 1 represents the highest observed value for each trait across genotypes; colour intensity reflects relative performance, with warmer colours indicating higher normalised values; GP – germination percentage (%); RL – root length (cm); SH – shoot height (cm); RFW – root fresh weight (g); SFW – shoot fresh weight (g); RDW – root dry weight (g); SDW – shoot dry weight (g)

mance across traits. Despite low germination, Aklei showed relatively greater root growth under stress conditions. Breeding materials 4a/1 and H1b2/12 maintained moderate and consistent performance, while Kamin excelled in root biomass but lagged in shoot growth.

Apparent accession-specific differences were observed in the normalised growth traits of *C. carvi*. Aprim and H1b2/12 showed the most balanced and relatively performance, with Aprim's excelling in germination (0.97), shoot height (1.00), and shoot fresh weight (0.68), while H1b2/12 achieved maximum values in germination (1.00), shoot fresh (0.92), and shoot dry weight (0.92), reflecting strong overall vigour and biomass efficiency. In contrast, Aklei and Kamin displayed root-oriented growth, as Aklei scored highest in root length (1.00) and root dry weight (1.00), and Kamin in root fresh weight (1.00) but remained low in other parameters. 4a/1 demonstrated moderate yet stable performance across traits, with notable shoot dry weight (1.00) (Figure 2).

The effect of PEG on growth parameters. The effects of different polyethylene glycol (PEG-6000) concentrations on the germination and early seedling growth parameters of *C. carvi* are shown in Figure 3. The results demonstrate a progressive decline in all measured traits with increasing PEG concentration. The GP exhibited a pronounced reduction, from 54.5% in the control (0% PEG) to 17.3% under 15% PEG, representing a 68% decrease. Similarly, RL and SH were highly sensitive to PEG-induced stress, decreasing steadily with increasing concentrations of PEG. Root length dropped from 4.65 cm in the control to 1.43 cm at 15% PEG. In comparison, shoot height declined from 2.88 cm to 1.00 cm. SFW decreased markedly from 11.59 g in control plants to 3.78 g at the highest PEG level, while RFW declined from 6.21 to 3.00 g.

A visual summary of how increasing PEG concentrations progressively suppress all growth parameters in *C. carvi* is shown in Figure 4. The control treatment (0% PEG) exhibited maximum normalised values (1.00) across all traits, confirming optimal germination and seedling growth under non-stress conditions. At 5% PEG, values moderately declined (0.63–0.91), indicating the onset of osmotic stress, yet with partial tolerance, particularly in root fresh weight (0.91). However, at 10% PEG, all parameters dropped sharply (0.26–0.50), reflecting substantial inhibition of germination and biomass accumulation. The most severe stress condition (15% PEG) completely suppressed all parameters (0.00), signifying a critical threshold where water potential becomes too low to sustain physiological activity.

Pearson correlation and PCA biplot analysis. The Pearson correlation matrix provides valuable insight

https://doi.org/10.17221/18/2026-CJGPB

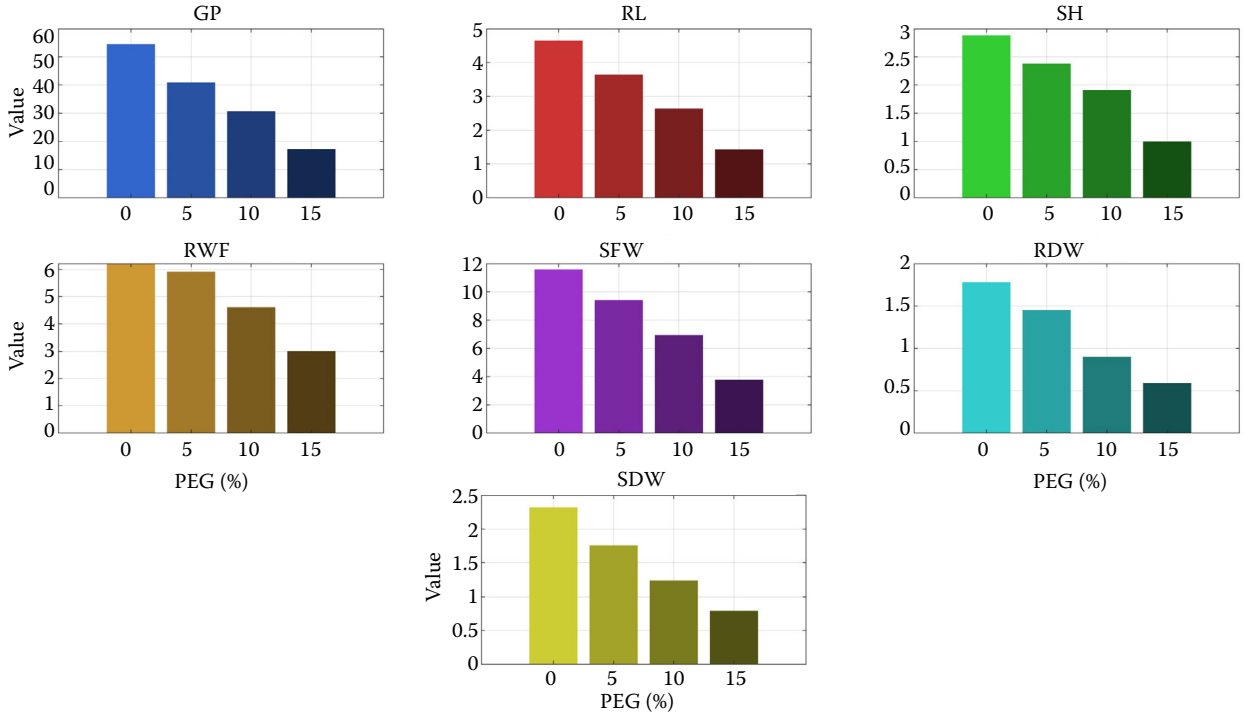

Figure 3. Effects of polyethylene glycol (PEG-6000) concentration on germination and seedling growth parameters of *Carum carvi*

Bars represent mean values averaged across all accessions for each PEG treatment; PEG concentrations are expressed as % (w/v); Germination percentage (%); GP – germination percentage (%); RL – root length (cm); SH – shoot height (cm); RFW – root fresh weight (g); SFW – shoot fresh weight (g); RDW – root dry weight (g); SDW – shoot dry weight (g)

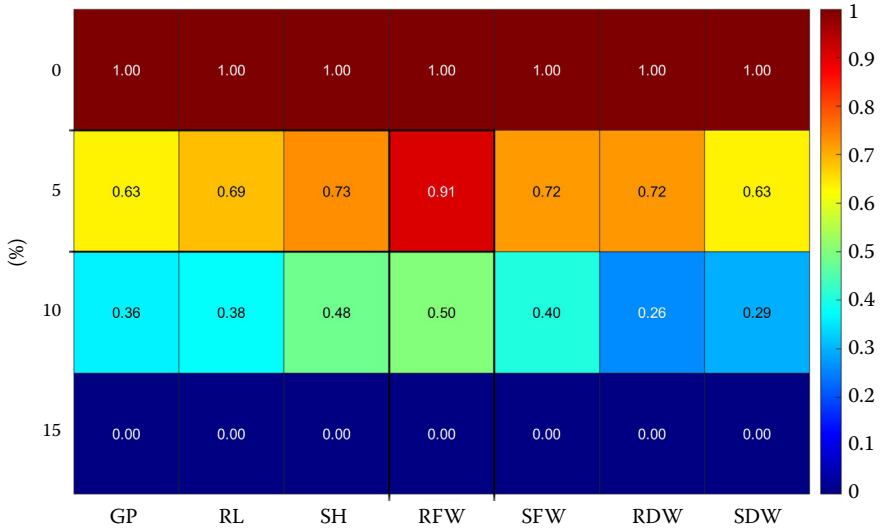

Figure 4. Normalised growth parameters of *Carum carvi* seedlings across polyethylene glycol (PEG-6000) concentrations; growth traits were normalised using min–max scaling (range: 0–1) to enable comparison among parameters with different units

Values are dimensionless, where 0 indicates the lowest and 1 indicates the highest observed value for each trait across PEG treatments; colour intensity reflects relative performance, with warmer colours indicating higher normalised values; PEG concentrations are expressed as % (w/v); GP – germination percentage (%); RL – root length (cm); SH – shoot height (cm); RFW – root fresh weight (g); SFW – shoot fresh weight (g); RDW – root dry weight (g); SDW – shoot dry weight (g)

https://doi.org/10.17221/18/2026-CJGPB

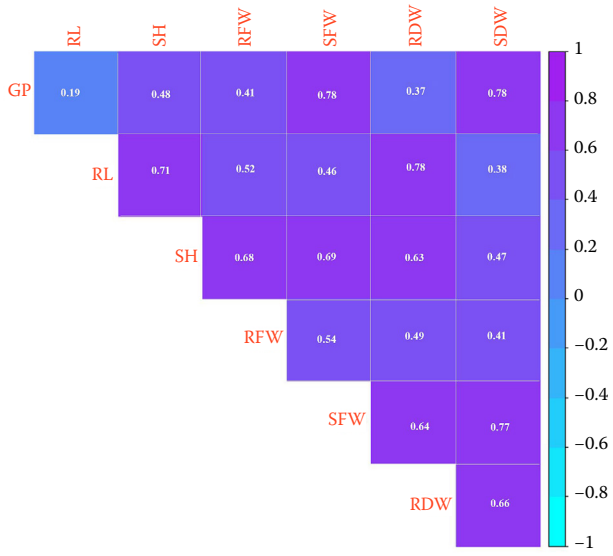

Figure 5. Pearson correlation matrix of germination and seedling growth parameters in *Carum carvi* under PEG-induced drought stress

Cells display Pearson correlation coefficients (*r*) calculated using pooled data across genotypes and PEG treatments; colour intensity represents the strength and direction of correlations, ranging from –1 (strong negative correlation) to +1 (strong positive correlation), as indicated by the colour scale; GP – germination percentage (%); RL – root length (cm); SH – shoot height (cm); RFW – root fresh weight (g); SFW – shoot fresh weight (g); RDW – root dry weight (g); SDW – shoot dry weight (g)

into the interrelationships among the measured growth parameters of *C. carvi* under PEG-induced drought stress (Figure 5). Most traits exhibited moderate to strong positive correlations. Germination showed positive but variable associations with other traits, being moderately correlated with shoot height (r = 0.48), shoot fresh weight (r = 0.78), and shoot dry weight (r = 0.78). However, there is a weak correlation between GP and root length (r = 0.19). Root length exhibited strong positive correlations with root dry weight (r = 0.78) and shoot height (r = 0.71), reflecting a balanced allocation between belowground and aboveground growth. Similarly, shoot height correlated strongly with shoot fresh weight (r = 0.69) and moderately with root dry weight (r = 0.63), highlighting the integrated nature of shoot and root biomass accumulation. The strongest associations were found between shoot fresh weight and shoot dry weight (r = 0.77) and between root dry weight and shoot dry weight (r = 0.66). The correlation matrix reveals a coherent growth pattern across parameters, where biomass-related traits (SFW, RDW, SDW) are tightly interlinked. At the same time, germination shows only indirect relationships with morphological and physiological performance.

The PCA biplot provides a multivariate overview of how the evaluated growth parameters contribute to the variation observed among *C. carvi* accessions under different PEG-induced drought stress conditions. The first two principal components (PC1 and PC2) accounted for 80% of the total variance, with PC1 explaining 63% and PC2 explaining 17%, indicating that most of the variability in the dataset can be summarised along these two axes (Figure 6).

Examination of the loading values (Table 2) shows that all measured traits contributed to PC1 with similar magnitude, indicating coordinated variation among growth parameters along this axis. In contrast, PC2 separated traits with different contributions, with RL, SH, RFW, and RDW showing positive loadings, while GP, SFW, and SDW exhibited negative loadings. The orientation of vectors in the biplot indicates associations among several traits, with RL, SH, RFW, and RDW pointing in similar directions, consistent with the correlations observed in the Pearson correlation analysis. GP displayed a different orientation relative to several growth parameters, reflecting its distinct contribution to PC2. The distribution of accessions across the PCA space shows variation among genotypes under PEG-induced stress conditions, with some accessions positioned closer to vectors representing elongation and biomass-related traits.

Machine learning analysis. The inclusion of the linear model provided an interpretable and data-appropriate baseline aligned with the factorial experi-

Table 2. Loading values of morphological traits contributing to the first two principal components (PC1 and PC2)

Trait	PC1	PC2
GP	–0.345	–0.568
RL	–0.345	0.542
SH	–0.400	0.247
RFW	–0.343	0.209
SFW	–0.423	–0.263
RDW	–0.394	0.249
SDW	–0.387	–0.385

GP – germination percentage; RL – root length; SH – shoot height; RFW – root fresh weight; SFW – shoot fresh weight; RDW – root dry weight; SDW – shoot dry weight

https://doi.org/10.17221/18/2026-CJGPB

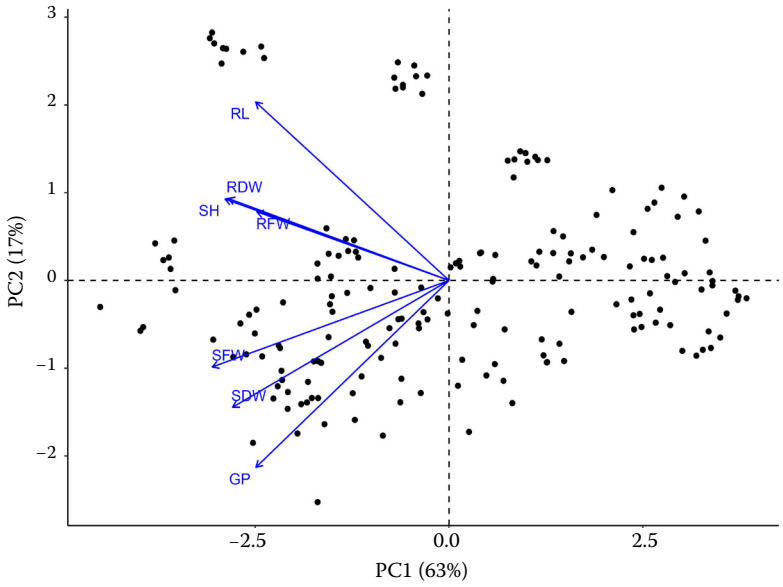

Figure 6. Principal component analysis (PCA) biplot of germination and seedling growth parameters of *Carum carvi* under PEG-induced drought stress

Black dots represent individual observations corresponding to accession × PEG treatment combinations; blue arrows indicate variable loadings, showing the direction and magnitude of each trait's contribution to the principal components; PC1 and PC2 explain 63% and 17% of the total variance, respectively; prior to PCA, all variables were standardised (mean = 0, variance = 1); GP – germination percentage (%); RL – root length (cm); SH – shoot height (cm); RFW – root fresh weight (g); SFW – shoot fresh weight (g); RDW – root dry weight (g); SDW – shoot dry weight (g)

Table 3. Illustrative prediction metrics for linear and machine-learning approaches applied to morphophysiological traits of *Carum carvi* seedlings; these metrics are provided for exploratory comparison only and should not be interpreted as evidence of model superiority

Parameters	Evaluation metrics	LM	MLP	QiMLP	SVR	QiSVR
GP	R^2	0.92	0.89	0.91	0.36	0.87
	RMSE	5.34	5.68	5.82	15.6	7.10
	MAE	3.76	4.30	4.18	12.4	4.51
RL	R^2	0.92	0.90	0.92	0.37	0.91
	RMSE	0.49	0.53	0.51	1.42	0.54
	MAE	0.35	0.34	0.35	1.08	0.37
SH	R^2	0.88	0.87	0.88	0.32	0.85
	RMSE	0.32	0.34	0.33	0.77	0.36
	MAE	0.24	0.26	0.25	0.62	0.27
RFW	R^2	0.81	0.80	0.82	0.27	0.81
	RMSE	0.83	0.79	0.79	1.59	0.82
	MAE	0.48	0.46	0.50	1.36	0.51
SFW	R^2	0.89	0.86	0.87	0.40	0.84
	RMSE	1.17	1.34	1.25	2.73	1.41
	MAE	0.66	0.72	0.75	2.15	0.85
RDW	R^2	0.92	0.91	0.93	0.53	0.91
	RMSE	0.15	0.17	0.15	0.38	0.17
	MAE	0.12	0.12	0.11	0.28	0.13
SDW	R^2	0.94	0.90	0.94	0.46	0.93
	RMSE	0.17	0.18	0.17	0.51	0.18
	MAE	0.13	0.14	0.13	0.40	0.14

R^2 – coefficient of determination; RSME – root mean squared error; MAE – mean absolute error; GP – germination percentage; RL – root length; SH – shoot height; RFW – root fresh weight; SFW – shoot fresh weight; RDW – root dry weight; SDW – shoot dry weight; LM – linear model; MLP – multilayer perceptron; QiMLP – quantum inspired multilayer perceptron; SVR – support vector regression; QiSVR – quantum inspired support vector regression

https://doi.org/10.17221/18/2026-CJGPB

mental design. Across all response variables, the LM demonstrated consistently high explanatory power, with R^2 values ranging from 0.81 to 0.94 (Table 3).

The performance comparison between conventional machine learning models (MLP, SVR) and their quantum-inspired counterparts (QiMLP, QiSVR) indicates that the integration of quantum-inspired mechanisms yielded broadly similar predictive performance, with minor numerical differences across the evaluated parameters (Table 3). For GP, the QiMLP and MLP produced comparable coefficients of determination (R^2 = 0.91 and 0.89, respectively), while QiSVR (R^2 = 0.87) showed notable improvement relative to classical SVR (R^2 = 0.36), which exhibited limited predictive capacity. Similar patterns emerged for RL and SH, where QiMLP yielded R^2 values of 0.92 and 0.88, respectively, with correspondingly low RMSE and MAE values. For biomass-related parameters such as RFW and SFW, QiMLP and MLP again produced closely aligned results (R^2 = 0.82 vs. 0.80 and 0.87 vs. 0.86, respectively), while QiSVR showed marginal improvement over classical SVR. For RDW and SDW, QiMLP attained R^2 values of 0.93 and 0.94, respectively, with RMSE values of 0.15 and 0.17 and MAE values of 0.11 and 0.13. Collectively, both conventional and quantum-inspired models exhibited broadly comparable predictive accuracy, and the observed numerical differences should be interpreted with caution, given the limited dataset size. The performance comparison between conventional and quantum-inspired architectures is illustrated in Figures 7–9, where QiMLP and QiSVR displayed generally consistent predictive behaviour, aligning closely with the 1 : 1 ideal fit line. The quantum-encoded feature visualisation (Figure 9) suggested that the trigonometric feature transformation may capture additional nonlinear structure in the data; however, its practical advantage over the linear model remains uncertain given the current dataset constraints.

The coefficient estimates (Figure 10) provide a detailed interpretation of the effects of PEG concentration, genotype, and their interaction on seedling traits. Across all traits, PEG concentration exhibited a consistently negative effect, particularly at higher levels

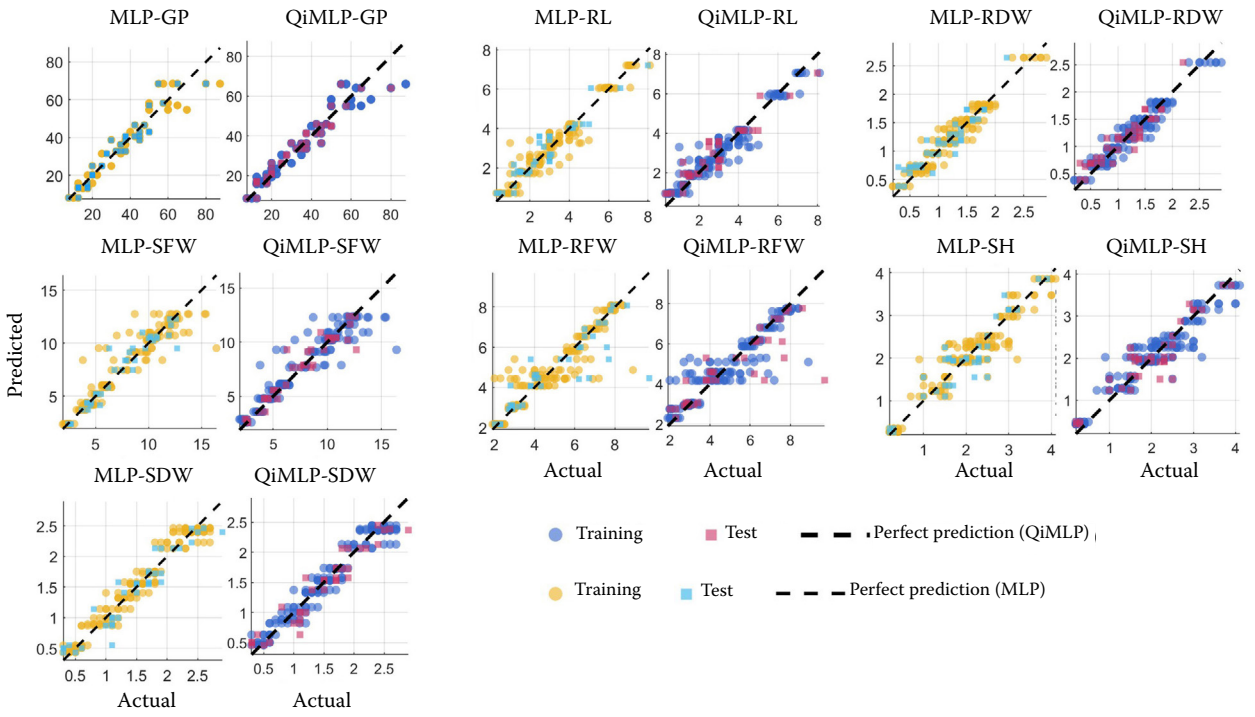

Figure 7. Comparison of actual and predicted values obtained using multilayer perceptron (MLP) and quantum-inspired multilayer perceptron (QiMLP) models for all target growth parameters of *Carum carvi*

Scatter plots show predicted values versus measured (actual) values for training and test datasets; the dashed diagonal line represents the 1 : 1 line corresponding to perfect prediction; all values are shown in original measurement units; GP – germination percentage (%); RL – root length (cm); RDW – root dry weight (g); SFW – shoot fresh weight (g); RFW – root fresh weight (g); SH – shoot height (cm); SDW – shoot dry weight (g)

https://doi.org/10.17221/18/2026-CJGPB

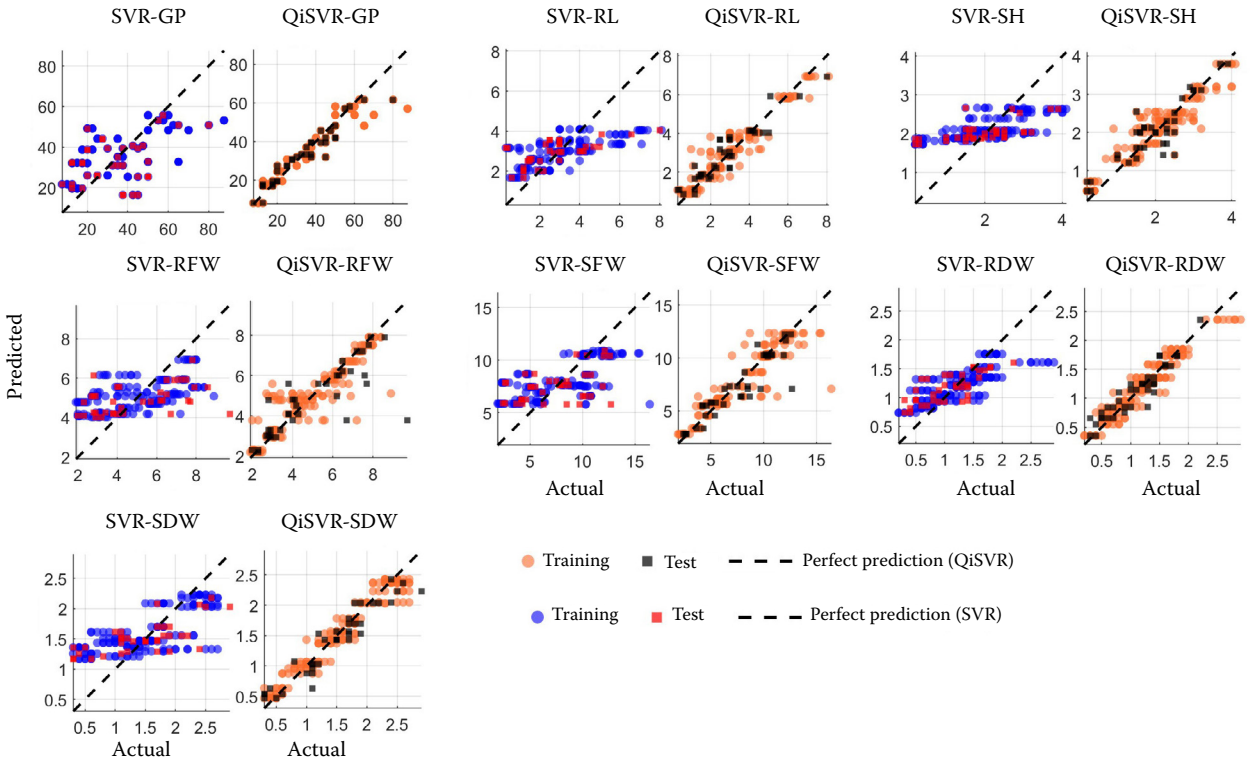

Figure 8. Comparison of actual and predicted values obtained using support vector regression (SVR) and quantum-inspired support vector regression (QiSVR) models for growth parameters of *Carum carvi*

Scatter plots show predicted values versus measured (actual) values for training and test datasets; the dashed diagonal line represents the 1 : 1 line corresponding to perfect prediction; all values are shown in original measurement units; GP – germination percentage (%); RL – root length (cm); SH – shoot height (cm); RFW – root fresh weight (g); SFW – shoot fresh weight (g); RDW – root dry weight (g); SDW – shoot dry weight (g)

(PEG 15%), confirming its strong inhibitory impact on germination and growth parameters. Genotype effects varied among accessions, indicating inherent differences in growth performance under control conditions. Notably, certain accessions showed positive baseline effects for biomass-related traits, while others exhibited lower initial performance. The interaction terms (PEG × genotype) revealed differential responses to drought stress among accessions. For example, some genotypes showed less negative or even partially positive interaction effects under moderate PEG levels.

DISCUSSION

Early seed germination and seedling establishment are highly sensitive to water deficit, making them critical stages that are often impaired under drought conditions (Li et al. 2013; Liang et al. 2025). Although the present study focused on morphological indicators of drought stress, these parameters alone cannot fully reveal the physiological mechanisms underlying stress tolerance. Measurements of physiological or biochemical markers such as proline accumulation, antioxidant enzyme activity, relative water content, or membrane stability index could provide deeper insight into the adaptive responses of different genotypes. Future studies integrating morphometric screening with physiological and molecular analyses would therefore help clarify the mechanisms associated with drought resilience in *C. carvi*.

In the present study, PEG-induced drought stress strongly inhibited *C. carvi* germination and seedling growth. The germination percentage plummeted by approximately 68% at the highest stress level (15% PEG) compared with that control conditions, reflecting the sharp reduction in seed water uptake and metabolic activation when the external water potential was low (Kebreab & Murdoch 1999; Al-

https://doi.org/10.17221/18/2026-CJGPB

len 2003; Hussain et al. 2018; Guo et al. 2024). This finding is consistent with general observations that drought stress leads to reduced seed imbibition, delayed or incomplete germination, and poor seedling vigour in many crops (Hussain et al. 2018). For example, in durum wheat, moderate osmotic stress may only delay germination, whereas more severe PEG-induced stress drastically lowers final germination rates. Our results align with these trends, as even mild PEG treatments (e.g., 5 % PEG) caused a significant decrease in *C. carvi* germination, and near-lethal osmotic stress (15% PEG, approximately –0.7 MPa) left only a small fraction of seeds able to germinate. Water stress not only delays the onset of germination but also prevents many seeds from ever emerging, a phenomenon documented in various species, including maize and sorghum, where increasing PEG levels progressively reduce germinated seed numbers, germination rate, and seedling vigour the number of germinated plants (Almansouri et al. 2001; Queiroz et al. 2019). Overall, the substantial decline in caraway germination under PEG confirms that adequate water potential is indispensable for seed activation, and even brief exposure to low water availability can severely curtail the transition from quiescent seeds to seedlings (Queiroz et al. 2019).

In addition to hindering germination, drought stress markedly suppressed early seedling growth

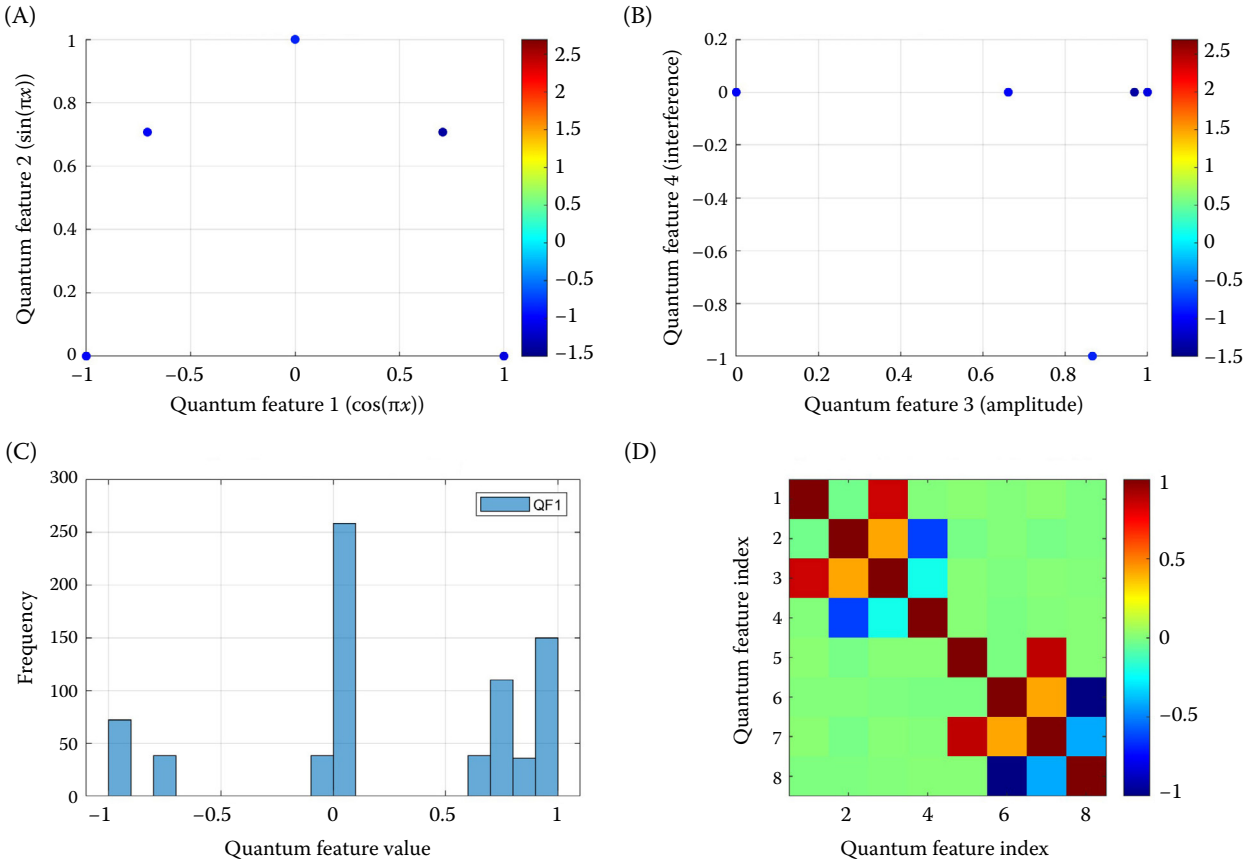

Figure 9. Conceptual and illustrative representation of the quantum-inspired feature transformations used in the exploratory analyses of *Carum carvi* growth traits; all panels represent classical nonlinear feature mappings and do not involve physical quantum hardware; this figure is included for methodological illustration only and is not required for the biological conclusions of the study: (A) quantum phase space representation of germination percentage (GP), where original input values are mapped into sinusoidal feature space using cosine and sine transformations, (B) quantum-inspired amplitude and interference feature space derived from nonlinear transformations of input variables, (C) distribution of quantum-inspired feature values (QF1), illustrating the range and frequency of transformed features, (D) correlation matrix of quantum-inspired features showing pairwise Pearson correlation coefficients; all quantum-inspired features are dimensionless and were used as input variables in the exploratory machine-learning analyses

https://doi.org/10.17221/18/2026-CJGPB

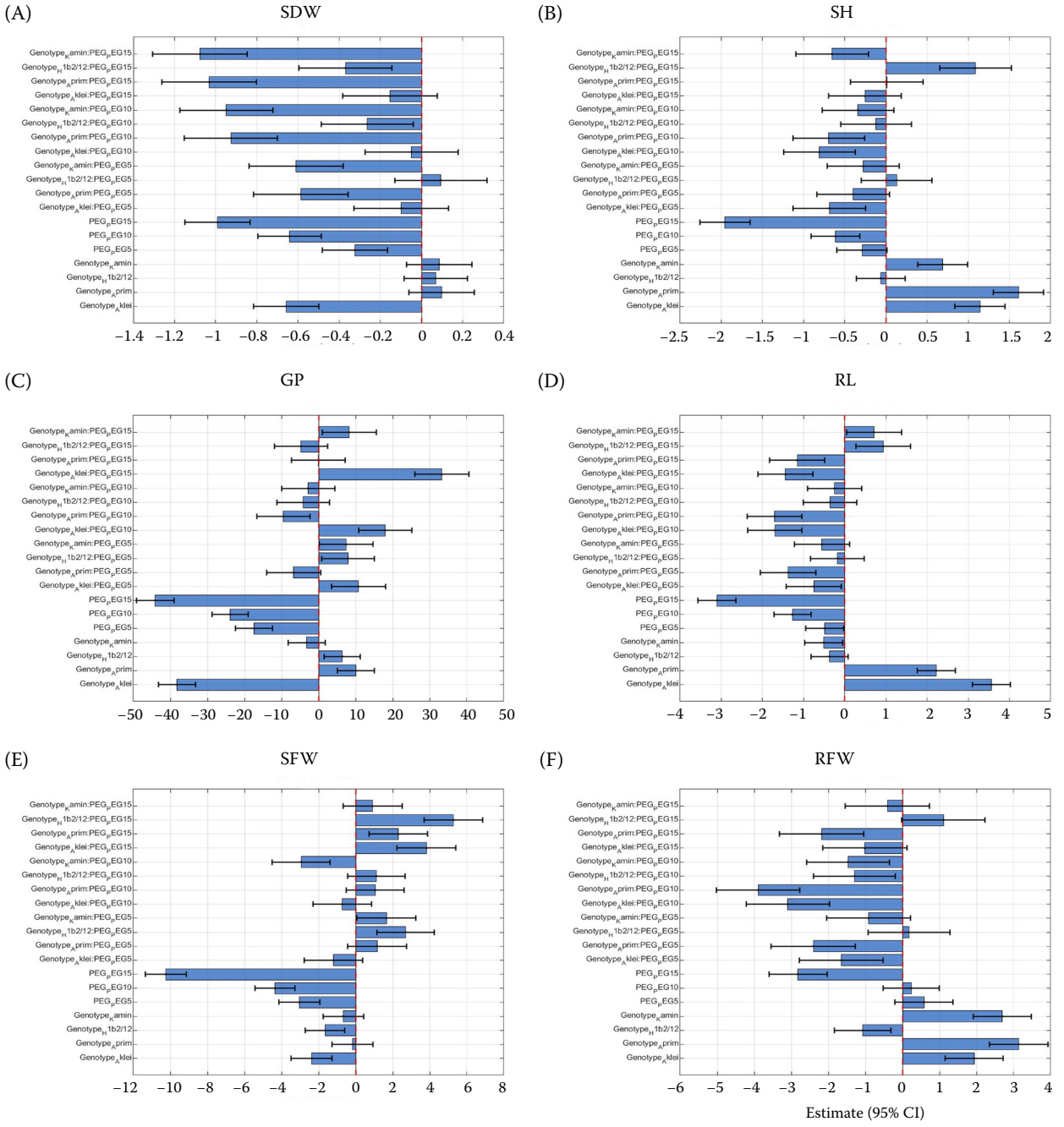

Figure 10. Coefficient estimates of linear models (LM) for morphophysiological traits of *Carum carvi* under PEG-induced drought stress: (A) SDW, (B) SH, (C) GP, (D) RL, (E) SFW, (F) RFW, and (G) RDW

Points indicate estimated coefficients, and horizontal bars represent 95% confidence intervals; the vertical dashed red line indicates zero effect; positive and negative coefficients reflect the direction and magnitude of PEG concentration, accession, and PEG × accession interaction effects on each trait
SDW – shoot dry weight; SH – shoot height; GP – germination percentage; RL – root length; SFW – shoot fresh weight; RFW – root fresh weight; RDW – root dry weight

https://doi.org/10.17221/18/2026-CJGPB

in caraway. We observed significant reductions in root length, shoot height, and biomass accumulation as the PEG concentration increased, indicating that osmotic stress inhibited cell expansion and elongation in both below- and above-ground organs. Notably, shoot growth was susceptible to water deficit; shoot height under severe stress was less than one-third that of control seedlings, which resulted from reduced turgor pressure and cell division under dehydration (Hussain et al. 2018). These observations align with classic principles of plant physiology: drought-induced low tissue water potential results in diminished cell enlargement, leading to stunted shoot development and smaller leaves (Khan et al. 2022). PEG also curtailed root growth, although in our study, the relative decrease in root length under moderate stress was slightly less pronounced than that observed in the shoots. This pattern suggests that caraway, like many other species, may prioritise root development under mild stress as a drought avoidance strategy. Indeed, an increased root-to-shoot ratio under water deficit is widely reported as an adaptive response, allowing plants to explore deeper or wider soil domains for water (Kou et al. 2022). In some crops, moderate osmotic stress can even stimulate slight root elongation as an adaptation; for example, specific pearl millet ecotypes presented increased root length at –1.0 MPa despite overall growth inhibition (Radhouane 2007). In our experiment, any compensatory root response was evident only at the lowest PEG level (5%, where the fresh weight of the roots decreased less sharply than the shoot mass), whereas at higher stress levels, all growth parameters uniformly collapsed. With 15% PEG, both root and shoot development were critically impaired (e.g., the root length decreased by ~70–80%, and the shoot height decreased by ~65% compared with that of the control), indicating that extreme osmotic stress overwhelmed the capacity of the seedlings to allocate biomass preferentially to the roots. These results underscore how drought stress not only reduces overall growth but also alters the balance of resource allocation between shoots and roots, especially under moderate stress conditions (Seleiman et al. 2021). The severe decreases in fresh and dry weights we recorded further reflect the cumulative impact of water scarcity on biomass production. Under drought, reduced water uptake likely limits photosynthetic activity and nutrient transport, resulting in lower dry matter accumulation (Hussain et al. 2018). Comparable magnitudes of biomass loss have been observed in other aromatic herbs; for example, in coriander, a 50% field capacity drought led to an approximately 50% reduction in shoot dry weight and fresh weight relative to those of well-watered plants (Khan et al. 2022). Similarly, drought-stressed fennel seedlings presented significantly lower fresh weights alongside signs of cellular injury, such as elevated membrane leakage (Seidler-Lozykowska et al. 2010; Farhoudi & Khordahampour 2017). In our caraway accessions, shoot fresh weight under severe PEG decreased by approximately 65–80% (depending on accession), paralleling these reports and confirming that water deficit drastically curtails biomass accumulation in Apiaceae seedlings. The increase in electrolyte leakage documented in related species under PEG stress (up to ~75% in fennel) suggests that dehydration may also cause membrane destabilization and oxidative damage in caraway tissues (Farhoudi & Khordahampour 2017). Although we did not measure biochemical markers in this study, it is likely that drought-induced oxidative stress was a contributing factor to growth inhibition, as has been reported in numerous plants under PEG treatment (e.g., increased lipid peroxidation and ROS formation leading to cell injury) (Hosseini et al. 2022). Overall, the strong dose-dependent decreases in germination, seedling length, and biomass observed in *C. carvi* confirm its sensitivity to osmotic drought stress and highlight the need for adequate moisture during early developmental stages (Li et al. 2013; Liang et al. 2025).

The pronounced genotypic variation observed in caraway is consistent with findings in other crops and medicinal plants. Drought tolerance is often genotype dependent, with some lines capable of maintaining better growth under stress due to inherent physiological and molecular traits. In our study, the difference between the most tolerant (Aprim) and most sensitive (Aklei) cultivars in terms of final germination at 15% PEG was on the order of 2.5-fold, and similar or greater ranges have been reported for related herbs. The severe inhibition observed at 15% PEG indicates that this treatment likely represents a near-threshold stress level for early seedling development in *C. carvi*. Such extreme osmotic conditions are commonly included in PEG-based screening experiments to identify tolerance limits and distinguish highly resilient genotypes from sensitive ones. Although this level may exceed typical field drought intensity, it provides a controlled means of evaluating physiological resilience during early developmental

https://doi.org/10.17221/18/2026-CJGPB

stages under standardised laboratory conditions. For example, a laboratory screening of coriander (*Coriandrum sativum*) genotypes under mild osmotic stress (–0.15 MPa PEG) revealed germination percentages ranging from 0% (no seeds germinated in more than half of the tested accessions) to approximately 27.5% in the best line (Kulkarni et al. 2014). This wide variability underscores the importance of genetic background: even under relatively modest drought stress, some coriander genotypes have completely failed to establish, whereas others have shown partial tolerance. In cumin (*Cumin cyminum*), which is often grown in arid climates, genotypic differences in seedling drought tolerance have also been documented (Neamatollahi et al. 2009), who reported that without any mitigation, cumin seeds exhibit drastically reduced germination as PEG-induced water stress increases, with virtually no germination occurring at approximately 20% PEG. Conversely, certain improved varieties of cumin have been bred for drought resilience (Arshadi-Bidgoli & Mortazavian 2025); for example, a newly developed drought-tolerant cumin cultivar was shown to germinate and grow more successfully under limited irrigation, which was attributed to traits such as efficient osmotic regulation and deeper rooting (Dorrani-Nejad et al. 2019). Similarly, in fennel (*Foeniculum vulgare*), genetic analyses indicate that drought stress causes a decline in most growth traits (plant height, branch number, etc.), but some genotypes respond by accumulating greater proline and maintaining a better harvest index, reflecting underlying tolerance mechanisms (Hosseini et al. 2022; Razavi et al. 2022). Even in major crops such as maize and wheat, researchers have reported that certain genotypes perform significantly better under PEG-simulated drought; for example, among several corn hybrids, one has the highest germination, root length, and seedling vigour under drought, indicating that it is the most tolerant hybrid (Queiroz et al. 2019). In wheat, the absence of drought-tolerant genotypes can severely limit production under water stress (Ahmed et al. 2025), which has driven extensive screening of diverse germplasms for germination and early growth traits under osmotic stress.

Collectively, these comparative insights reinforce that the variability we observed in caraway is not an outlier; drought tolerance tends to segregate among accessions in many species, including close relatives in the Apiaceae family (coriander, cumin, and fennel) as well as staple crops. This highlights the importance of identifying and propagating drought-tolerant caraway accessions. In practical terms, accessions such as Aprim and H1b2/12 (which presented greater germination and biomass under stress in our study) could be promising candidates for cultivation in drought-prone regions or for use as parents in breeding programs aiming to improve the drought resilience of caraway in Czechia regions, which are affected by severe drought. Moreover, the pronounced root elongation observed in Aklei may indicate a tendency toward root-oriented growth under stress conditions. Such responses are sometimes associated with drought avoidance strategies; however, additional physiological measurements would be required to determine whether this pattern reflects adaptive stress tolerance or simply a growth allocation trade-off. In summary, our genotypic results, in accordance with other crop data, highlight that substantial intraspecific variation exists in the drought response. Leveraging this variation is crucial for improving the drought tolerance of caraway through genetic selection and agronomic management.

It should also be noted that variation in germination percentage among accessions under control conditions may partly reflect inherent genetic differences in seed vigour. Although all seeds originated from the same breeding source and were stored under standardised conditions, additional seed viability assessments (e.g., tetrazolium staining or standardised germination tests) could further confirm baseline seed quality in future studies. In addition, PEG-induced osmotic stress represents a controlled laboratory simulation of water deficit and does not fully replicate the complexity of soil-based drought conditions, including root–soil interactions and fluctuating water availability. Therefore, the results should be interpreted as indicators of early-stage stress responses under controlled conditions rather than direct representations of field drought performance.

The application of ML in plant science has revolutionised the prediction of complex morphophysiological traits, moving beyond traditional statistical analyses (Bektaş et al. 2024). In our study, classical models (MLP, SVR) were benchmarked against their quantum-inspired counterparts (QiMLP, QiSVR). The classical MLP model demonstrated strong predictive capability (R^2 = 0.80–0.91), confirming its established utility in plant phenotyping. Importantly, the linear model (LM) performed comparably to the ML approaches for most traits (R^2 = 0.81–0.94), confirming

https://doi.org/10.17221/18/2026-CJGPB

that the dominant variation in this controlled factorial experiment is well captured by classical statistical methods. The quantum-inspired variants showed numerically similar or modestly different metrics compared to their classical counterparts, although such differences should be interpreted cautiously given the limited sample size. The largest contrast was observed between SVR and QiSVR, where the enriched feature space appeared to improve model fit, though this may partly reflect the sensitivity of SVR to input representation rather than a genuine advantage of quantum-inspired approaches that would generalise to larger datasets. Similarly, the QiMLP model yielded numerically high R^2 values, but the margins over the LM and classical MLP were small and do not support claims of clear superiority (R^2 up to 0.94). These results are broadly consistent with the linear model and do not indicate a clear practical advantage of quantum-inspired encoding for this dataset. Nonetheless, emerging literature has explored quantum and quantum-inspired approaches for plant phenotyping tasks. For example, studies on woody shrubs such as *Aronia melanocarpa*, *Lycium barbarum*, and *Olea europaea* have successfully employed classical algorithms like random forest (RF) and XGBoost to predict in vitro regeneration and stress responses with high accuracy ($R^2 > 0.95$) (Isak et al. 2024; Palaz et al. 2025; Yaman et al. 2025). Some recent studies have reported that quantum-inspired models can in certain cases complement these classical benchmarks. For instance, Katırcı et al. (2025) reported that a custom quantum circuit achieved an accuracy of 83% for shoot regeneration in common bean, significantly outperforming a classical support vector classifier (67%). Similarly, Alshahrani et al. (2023) demonstrated that a quantum-inspired moth flame optimizer (QIMFO) enhanced deep learning models to achieve 99.66 % accuracy in rice variety classification, surpassing the accuracy of standard CNNs.

The specific advantage of our QiSVR model mirrors findings by Anand et al. (2025), who utilized quantum convolutional neural networks (QCNN) for plant disease prediction. They found that quantum-derived features allowed for an accuracy of ~80–82%, outperforming classical deep learning models (~75%) by effectively managing high-dimensional feature spaces. Furthermore, while Katırcı et al. (2024) observed that classical MLP could still outperform quantum models (VQC) in overall accuracy for cowpea regeneration, they noted that quantum models offered superior recall (100%) and sensitivity. In our study, however, the linear model captured the dominant patterns of variation as effectively as the ML models, suggesting that for controlled factorial experiments with limited sample sizes, quantum-inspired feature transformations may offer a complementary, though not necessarily superior, approach to classical methods, particularly when modelling the non-linear plasticity of plant growth under stress. Future studies incorporating individual-seed measurements could substantially increase dataset size and provide a stronger foundation for machine-learning-based modelling approaches. Expanding the dataset and exploring additional modelling frameworks, such as ensemble methods, mixed-effects models, or cross-validated machine learning techniques, may further improve predictive robustness and provide deeper insight into the structure of drought-response traits. From an applied perspective, the modelling framework may support early-stage screening by enabling rapid ranking of accessions according to predicted growth responses under different osmotic stress levels. Such predictive models may also assist exploratory scenario testing, allowing researchers to estimate how different accessions might respond to varying drought intensities before conducting more extensive physiological or field evaluations. From a breeding perspective, the observed variation among accessions in germination, root development, and biomass accumulation under PEG-induced stress provides valuable insight into early-stage drought tolerance. Accessions such as Aprim and H1b2/12 demonstrated relatively stable performance across stress levels, suggesting their potential suitability for selection in drought-prone environments. In contrast, accessions exhibiting strong reductions in growth parameters may be considered more sensitive and less suitable for water-limited conditions. These findings highlight the importance of early-stage phenotyping for identifying genotypes with improved stress resilience.

CONCLUSION

This study shows that PEG-induced osmotic stress significantly limits germination, root-shoot growth, and biomass accumulation in *C. carvi*, with responses varying among accessions. Aprim and H1b2/12 consistently maintained better vigour under increasing drought conditions, while Aklei adopted a different strategy marked by low germination but substantial root growth. These accession-specific patterns were

https://doi.org/10.17221/18/2026-CJGPB

further supported by multivariate analyses, which revealed coordinated decreases in biomass-related traits and differentiation in early-stage stress responses among accessions. Machine-learning approaches offered complementary insights into trait relationships, but these results should be interpreted cautiously, given the limited dataset size. Importantly, the biological conclusions regarding drought response and accession performance are fully supported by the linear model and do not depend on the exploratory ML analyses.

REFERENCES

Agnihotri V., Shashni S., Tripathi M. (2024): Morphological, phytochemical and pharmacological properties of *Carum carvi* (caraway) and *Bunium persicum* (black caraway) seeds: A review. Journal of Food Engineering and Technology, 13: 25–31.

Ahluwalia O., Singh P.C., Bhatia R. (2021): A review on drought stress in plants: Implications, mitigation and the role of plant growth promoting rhizobacteria. Resources, Environment and Sustainability, 5: 100032.

Ahmed K., Shabbir G., Ahmed M. (2025): Exploring drought tolerance for germination traits of diverse wheat genotypes at seedling stage: A multivariate analysis approach. BMC Plant Biology, 25: 390.

Allen P.S. (2003): When and how many? Hydrothermal models and the prediction of seed germination. New Phytologist, 158: 1–3.

Almaghrabi O.A. (2012): Impact of drought stress on germination and seedling growth parameters of some wheat cultivars. Journal of Agricultural Science, 4: 1–9.

Almansouri M., Kinet J.-M., Lutts S. (2001): Effect of salt and osmotic stresses on germination in durum wheat (*Triticum durum* Desf.). Plant and Soil, 231: 243–254.

Alshahrani H.M., Saeed M.K., Alotaibi S.S., Mohamed A., Assiri M., Ibrahim S.S. (2023): Quantum-inspired moth flame optimizer enhanced deep learning for automated rice variety classification. IEEE Access, 11: 125593–125600.

Aly A., Maraei R., Rezk A., Diab A. (2023): Phytochemical constituents and biological activities of essential oil extracted from irradiated caraway seeds (*Carum carvi* L.). International Journal of Radiation Biology, 99: 318–328.

Anand K., Jain B., Mittal H., Yadav V.K. (2025): QEFS: A novel plant disease prediction approach using quantum-inspired evolutionary feature selection. Applied Intelligence, 55: 101–115.

Arshadi-Bidgoli M., Mortazavian S.M.M. (2025): Polycross breeding enhances cumin quality and drought tolerance for sustainable agriculture. Scientific Reports, 15: 18927.

Bailer J., Aichinger T., Hackl G., de Hueber K., Dachler M. (2001): Essential oil content and composition in commercially available dill cultivars in comparison to caraway. Industrial Crops and Products, 14: 229–239.

Bayoumi T.Y., Eid M.H., Metwali E.M. (2008): Application of physiological and biochemical indices as a screening technique for drought tolerance in wheat genotypes. African Journal of Biotechnology, 7: 2341–2352.

Bektaş Ü., Isak M.A., Bozkurt T., Dönmez D., İzgü T., Tütüncü M., Şimşek Ö. (2024): Genotype-specific responses to in vitro drought stress in myrtle (*Myrtus communis* L.): Integrating machine learning techniques. PeerJ, 12: e18081.

Bouwmeester H.J., Smid H.G. (1995): Seed yield in caraway (*Carum carvi*). 1. Role of pollination. The Journal of Agricultural Science, 124: 235–244.

Dorrani-Nejad M., Aghighi S., Mohammadi-Nejad G. (2019): Evaluation of elite genotypes for drought tolerance in cumin (*Cuminum cyminum* L.) using drought tolerance indices. Plant Productions, 42: 227–238.

Ema R.M., Samad R., Mohtasim M., Islam T. (2025): Physiological, biochemical, and molecular analysis of PEG-induced water stress responses in lentil (*Lens culinaris* Medik.). Journal of Plant Nutrition, 48: 2019–2036.

Farhoudi R., Khordahampour Z. (2017): Effect of salt and drought stresses on germination, seedling growth and cell membrane stability of anise (*Pimpinella anisum*) and fennel (*Foeniculum vulgare*). Journal of Plant Process and Function, 5: 10–17.

Guo M., Zong J., Zhang J., Wei L., Wei W., Fan R., Zhang T., Tang Z., Zhang G. (2024): Effects of temperature and drought stress on seed germination of a peatland lily (*Lilium concolor* var. *megalanthum*). Frontiers in Plant Science, 15: 1462655.

Hosseini E., Majidi M.M., Saeidnia F., Ehtemam M.H. (2022): Genetic analysis and physiological relationships of drought response in fennel. PLoS ONE, 17: e0277926.

Hussain H.A., Hussain S., Khaliq A., Ashraf U., Anjum S.A., Men S., Wang L. (2018): Chilling and drought stresses in crop plants: Implications, cross talk, and management opportunities. Frontiers in Plant Science, 9: 393.

Isak M.A., Bozkurt T., Tütüncü M., Dönmez D., İzgü T., Şimşek Ö. (2024): Leveraging machine learning to unravel the impact of cadmium stress on goji berry micropropagation. PLoS ONE, 19: e0305111.

Kamilaris A., Prenafeta-Boldú F.X. (2018): A review of the use of convolutional neural networks in agriculture. The Journal of Agricultural Science, 156: 312–322.

Katırcı R., Aasim M., Deveci G., Mustafa Z. (2024): Comparing quantum machine learning and classical machine

https://doi.org/10.17221/18/2026-CJGPB

learning for in vitro regeneration of cowpea (*Vigna unguiculata*). Plant Cell, Tissue and Organ Culture, 159: 32.

Katırcı R., Aasim M., Aadil F., Chohan R.T. (2025): Quantum machine learning–driven optimization of nutrient–hormone interactions for enhanced in vitro regeneration of common bean. BMC Plant Biology, 25: 1575.

Kaya M.D., Okçu G., Atak M., Çikili Y., Kolsarici Ö. (2006): Seed treatments to overcome salt and drought stress during germination in sunflower. European Journal of Agronomy, 24: 291–295.

Kebreab E., Murdoch A.J. (1999): Modeling the effects of water stress and temperature on germination rate of *Orobanche aegyptiaca* seeds. Journal of Experimental Botany, 50: 655–664.

Khan M.T., Ahmed S., Sardar R., Shareef M., Abbasi A., Mohiuddin M., Ercisli S., Fiaz S., Marc R.A., Attia K. (2022): Impression of foliar-applied folic acid on coriander (*Coriandrum sativum* L.) under drought stress. Frontiers in Plant Science, 13: 1005710.

Kou X., Han W., Kang J. (2022): Responses of root system architecture to water stress at multiple levels: A meta-analysis. Frontiers in Plant Science, 13: 1085409.

Kulkarni S., Hongal S., Shoba N. (2014): Standardization of optimal concentration of PEG 6000 for induction of drought and screening of coriander (*Coriandrum sativum* L.) genotypes. The Asian Journal of Horticulture, 9: 100–105.

Laribi B., Bettaieb I., Kouki K., Sahli A., Mougou A., Marzouk B. (2009): Water deficit effects on caraway: Growth, essential oil and fatty acid composition. Industrial Crops and Products, 30: 372–379.

Li H., Li X., Zhang D., Liu H., Guan K. (2013): Effects of drought stress on seed germination and early seedling growth of the desert plant *Eremosparton songoricum*. EXCLI Journal, 12: 89–98.

Liakos K.G., Busato P., Moshou D., Pearson S., Bochtis D. (2018): Machine learning in agriculture: A review. Sensors, 18: 2674.

Liang Cai B., Zhu Z., Liu T., Hui Wang J., Tian Q. (2025): The effects of drought stress on seed germination and seedling physiology of three *Limonium* species. Scientia Horticulturae, 351: 114396.

Licaj I., Fiorillo A., Di Meo M.C., Varricchio E., Rocco M. (2024): Effect of polyethylene glycol-simulated drought stress on stomatal opening in "modern" and "ancient" wheat varieties. Plants, 13: 1575.

Mirmazloum I., Kiss A., Erdélyi É., Ladányi M., Németh É.Z., Radácsi P. (2020): The effect of osmopriming on seed germination and early seedling characteristics of *Carum carvi* L. Agriculture, 10: 94.

Mittler R., Karlova R., Bassham D.C., Lawson T. (2025): Crops under stress: can we mitigate the impacts of climate change on agriculture and launch the 'Resilience Revolution'? Philosophical Transactions of the Royal Society B: Biological Sciences, 380: 20240228.

Money N.P. (1989): Osmotic pressure of aqueous polyethylene glycols: Relationship between molecular weight and vapor pressure deficit. Plant Physiology, 91: 766–769.

Neamatollahi E., Bannayan M., Darban A.S., Ghanbari A. (2009): Hydropriming and osmopriming effects on cumin seeds. World Academy of Science, Engineering and Technology, 57: 526–529.

Nezamivand C.R., Benakashani F., Alahdadi I., Soltani E. (2021): Quantification of salinity and drought effects on fourteen ecotypes of black caraway (*Nigella sativa* L.). Environmental Stresses in Crop Sciences, 14: 211–220.

Othmani A., Ayed S., Chamekh Z., Slama-Ayed O., Da Silva J.A.T., Rezgui M., Slim-Amara H., Younes M.B. (2021): Screening seedlings of durum wheat cultivars for tolerance to PEG-induced drought stress. Pakistan Journal of Botany, 53: 823–832.

Palaz E.B., Demirel S., Popescu G.C., Demirel F., Uğur R., Yaman M., Tunç Y. (2025): Refinement of surface sterilization protocol for in vitro olive (*Olea europaea* L.) shoot proliferation and optimization by machine learning techniques. Horticulture, Environment, and Biotechnology, 66: 813–828.

Queiroz M.S., Oliveira C.E., Steiner F., Zuffo A.M., Zoz T., Vendruscolo E.P., Silva M.V., Mello B., Cabral R.C., Menis F.T. (2019): Drought stresses on seed germination and early growth of maize and sorghum. Journal of Agricultural Science, 11: 310–318.

Radhouane L. (2007). Response of Tunisian autochthonous pearl millet (*Pennisetum glaucum* L.) to drought stress induced by polyethylene glycol 6000. African Journal of Biotechnology, 6: 964–969.

Rasooli I., Allameh A. (2016): Caraway (*Carum carvi* L.) essential oils. In: Preedy V.R. (ed.): Essential Oils in Food Preservation, Flavor and Safety. Amsterdam, Academic Press: 287–293.

Razavi S.M., Ghorbanian A., Abadi A. (2022): Impact of drought stress on growth–yield parameters, volatile constituents and physio-biochemical traits of three *Foeniculum vulgare* genotypes. Agricultural Research, 11: 591–607.

Rezaei H., Mirzaie-Asl A., Abdollahi M.R., Tohidfar M. (2023): Comparative analysis of different artificial neural networks for predicting and optimizing in vitro seed germination and sterilization of petunia. PLoS ONE, 18: e0285657.

Seidler-Lozykowska K., Bandurska H., Bocianowski J. (2010): Evaluation of cell membrane injury in caraway

https://doi.org/10.17221/18/2026-CJGPB

genotypes under water deficit conditions. Acta Societatis Botanicorum Poloniae, 79: 95–99.

Seleiman M.F., Al-Suhaibani N., Ali N., Akmal M., Alotaibi M., Refay Y., Dindaroglu T., Abdul-Wajid H., Battaglia M.L. (2021): Drought stress impacts on plants and different approaches to alleviate its adverse effects. Plants, 10: 259.

Sharma V., Kumar A., Chaudhary A., Mishra A., Rawat S., Basavaraj Y.B., Shami V., Kaushik P. (2022): Response of wheat genotypes to drought stress stimulated by PEG. Stresses, 2: 26–51.

Şimşek Ö. (2024): Machine learning offers insights into the impact of in vitro drought stress on strawberry cultivars. Agriculture, 14: 294.

Valkovszki N., Németh-Zámbori É. (2011): Effects of growing conditions on essential oil content and composition of annual caraway (*Carum carvi* L. var. *annua*). Acta Alimentaria, 40: 235–246.

Verslues P.E., Agarwal M., Katiyar-Agarwal S., Zhu J., Zhu J.K. (2006): Methods and concepts in quantifying resistance to drought, salt and freezing, abiotic stresses that affect plant water status. The Plant Journal, 45: 523–539.

von Maydell D., Lehnert H., Berner T., Klocke E., Junghanns W., Keilwagen J., Marthe F. (2020): On genetic diversity in caraway: Genotyping of a large germplasm collection. PLoS ONE, 15: e0244666.

Yaman M., Palaz E.B., Isak M.A., Demirel S., İzgü T., Adalı S., Popescu M. (2025): Integrating *in vitro* propagation and machine learning modeling for efficient shoot and root development in *Aronia melanocarpa*. Horticulturae, 11: 886.

Zarbakhsh S., Shahsavar A.R., Soltani M. (2024): Optimizing PGRs for *in vitro* shoot proliferation of pomegranate with Bayesian-tuned ensemble stacking regression and NSGA-II: a comparative evaluation of machine learning models. Plant Methods, 20: 82.

Zhang J., Wang T., Zhang Z., Yan P., Li X. (2025): QiMLP: Quantum-inspired multilayer perceptron with strong correlation mining and parameter compression. Proceedings of the AAAI Conference on Artificial Intelligence, 39: 22452–22460.

Received: February 10, 2026
Accepted: May 11, 2026
Published online: May 26, 2026